Dextran hydrogel scaffolds enhance angiogenic responses and promote complete skin regeneration during burn wound healing

Guoming Sun[a], Xianjie Zhang[b], Yu-I Shen[a], Raul Sebastian[b], Laura E. Dickinson[a], Karen Fox-Talbot[c], Maura Reinblatt[b], Charles Steenbergen[c], John W. Harmon[b], and Sharon Gerecht[a,1]

[a]Department of Chemical and Biomolecular Engineering, Johns Hopkins Physical Sciences–Oncology Center, and the Institute for NanoBioTechnology, The Johns Hopkins University, Baltimore, MD 21218; [b]Department of Surgery and the Hendrix Burn Lab, The Johns Hopkins University School of Medicine, Baltimore, MD 21224; and [c]Department of Pathology, The Johns Hopkins University School of Medicine, Baltimore, MD 21287

Edited by Robert Langer, Massachusetts Institute of Technology, Cambridge, MA, and approved October 25, 2011 (received for review September 30, 2011)

Neovascularization is a critical determinant of wound-healing outcomes for deep burn injuries. We hypothesize that dextran-based hydrogels can serve as instructive scaffolds to promote neovascularization and skin regeneration in third-degree burn wounds. Dextran hydrogels are soft and pliable, offering opportunities to improve the management of burn wound treatment. We first developed a procedure to treat burn wounds on mice with dextran hydrogels. In this procedure, we followed clinical practice of wound excision to remove full-thickness burned skin, and then covered the wound with the dextran hydrogel and a dressing layer. Our procedure allows the hydrogel to remain intact and securely in place during the entire healing period, thus offering opportunities to simplify the management of burn wound treatment. A 3-week comparative study indicated that dextran hydrogel promoted dermal regeneration with complete skin appendages. The hydrogel scaffold facilitated early inflammatory cell infiltration that led to its rapid degradation, promoting the infiltration of angiogenic cells into the healing wounds. Endothelial cells homed into the hydrogel scaffolds to enable neovascularization by day 7, resulting in an increased blood flow significantly greater than treated and untreated controls. By day 21, burn wounds treated with hydrogel developed a mature epithelial structure with hair follicles and sebaceous glands. After 5 weeks of treatment, the hydrogel scaffolds promoted new hair growth and epidermal morphology and thickness similar to normal mouse skin. Collectively, our evidence shows that customized dextran-based hydrogel alone, with no additional growth factors, cytokines, or cells, promoted remarkable neovascularization and skin regeneration and may lead to novel treatments for dermal wounds.

Burn injuries constitute a major worldwide public health problem (1) and cause more severe physiological stress than other traumas (2, 3). Superficial burns usually heal with minimal scarring, but treatments for second- and third-degree burn injuries remain far from optimal (1, 4). Burn-induced full-thickness skin injuries result in rapid and dangerous liquid loss and impair many vital functions that skin performs. The healing process for adult skin wounds is complex, requiring the collaborative efforts of various tissues and cell lineages, as well as both extracellular and intracellular signals (5, 6). Although research has elucidated many details of the basic wound-healing process (7), the regeneration of perfect skin remains an elusive goal (8).

Third-degree burns involve damage to both epidermal and dermal layers and may also cause damage to underlying muscles, bones, and tendons. Such burns heal with thick scars, resulting in contractures that distort the surrounding tissue. Deep third-degree burns usually require skin grafting to achieve wound closure, but the cosmetic and functional results are less than optimal, as the grafted skin is thin and vulnerable to reinjury. In general, wound repair has three classic stages: the inflammatory, proliferative, and remodeling stages (6, 9, 10). The inflammatory stage begins with hemostasis and formation of the platelet plug. Platelets release growth factors to attract neutrophils and macrophages (11). Neutrophil influx, an early inflammatory response, is essential for the clearance of bacteria and both cellular and foreign debris (12), whereas macrophages produce growth factors that induce and accelerate angiogenesis during wound healing (13). The inflammatory stage overlaps with the proliferative stage where an eschar forms on the surface of the wound. In the proliferative stage, most cells from the inflammatory stage of repair have disappeared from the wound, and new blood vessels now populate the area (6). Initiation of the remodeling stage occurs when collagen formation and breakdown reach a state of equilibrium. In this stage, fibroblasts that have migrated into the wound lay down disorganized collagen, and fibroblasts differentiate into myofibroblasts, causing tissue contraction. Collagen reorganizes along lines of tension and cross-links, giving additional strength. Nevertheless, wounds are unable to attain the same mechanical strength as uninjured skin (14).

Angiogenesis and neovascularization are critical determinants of the wound-healing outcomes for deep burn injuries (15). Severe burn wounds lose more dermal blood flow than superficial burns. Newly formed blood vessels participate in the healing process, providing nutrition and oxygen to growing tissues (7). The repair of the dermal vasculature largely determines whether second-degree burns heal promptly and primarily or, due to delayed healing, they become third-degree burns, with the consequent necrosis and damaging scarring. Thus, encouraging angiogenesis could promote dermal layer regeneration and complete skin formation. Hydrogels, structurally similar to the natural extracellular matrix, can be designed to provide instructive environments for the three-dimensional assembly of vascular networks. Many studies of hydrogel-based scaffolds have focused on applications in healing wounds (5, 16–21). Beyond their utility as scaffolds, hydrogels can also deliver cytokines and growth factors (22, 23), antibiotics (20), and cells (24, 25) to allow complete skin regeneration.

Recent efforts in our laboratory have focused on tailoring the properties of chemically modified dextran hydrogels to promote rapid, functional neovascularization in vivo. We first demonstrated that the incorporation of functional groups—specifically, amine groups—into dextran hydrogel scaffolds enhanced biocompatibility and integration with the host tissue (26). To promote tissue infiltration, neovascularization, and hydrogel degradation, we modified the physical properties of the dextran hydrogels by redu-

Author contributions: G.S., X.Z., M.R., J.W.H., and S.G. designed research; G.S., X.Z., Y.-I.S., R.S., and L.E.D. performed research; G.S., Y.-I.S., R.S., K.F.-T., C.S., J.W.H., and S.G. analyzed data; and G.S., L.E.D., C.S., J.W.H., and S.G. wrote the paper.

The authors declare no conflict of interest.

This article is a PNAS Direct Submission.

[1]To whom correspondence should be addressed. E-mail: gerecht@jhu.edu.

This article contains supporting information online at www.pnas.org/lookup/suppl/doi:10.1073/pnas.1115973108/-/DCSupplemental.

cing the degree of substitution of cross-linking groups. This generated a hydrogel, dextran-allyl isocyanate-ethylamine (Dex-AE)/polyethylene glycol diacrylate (PEGDA) in ratio of 80/20, exhibiting a loose interior architecture but mechanically durable to enable ease of management for transplantation (27). In this study, we reasoned that stimulating rapid neovascularization through the material-tissue interaction would enhance the burn wound-healing process, resulting in skin regeneration. Toward this end, we sought to determine if the newly developed dextran hydrogels could serve as burn wound scaffolds to promote healing (Fig. 1*A*). An ideal wound scaffold should protect the wound from bacterial infection, control evaporative water loss and prevent dehydration, allow diffusion of oxygen and carbon dioxide, absorb wound exudate, and enhance healing (5). For third-degree burn injuries, the wound scaffold should also promote angiogenesis to achieve a favorable healing result. Hence, for viable translational outcomes, we considered that dextran hydrogel alone, with no additional growth factors, cytokines, or cells, would prove sufficient to treat wound injuries.

We have utilized a previously established murine burn wound model (1, 4, 28). An important improvement in treating deep burn injuries is to remove badly burned skin followed by the application of wound dressing matrix (i.e., artificial skin), which offers greater protection against wound infection and improves the prognosis of severely burned patients (29). In pursuit of translational outcomes, we developed a procedure for applying dextran hydrogels onto burn wounds in mice; we designed this procedure that follows clinical setting of wound excision 48 h after the burn. We removed full-thickness skin from the center of the wound (approximately 8 mm) leaving a small (approximately 2 mm) rim of burned tissue around the excision. The wound was then covered with the same size of hydrogel, and layered with DuoDerm®, an extra thin dressing, to enable hydrogel placement, protect it from infection, and prevent it from drying (Fig. S1*A*). Our procedure leaves the hydrogel intact and in place for the entire healing period, thus offering opportunities to simplify the management of burn wound treatment. For comparison purposes, we applied Integra®, a cross-linked bovine tendon collagen and glycosaminoglycan matrix, which is the state-of-the-art treatment currently used for patients with deep burns at the Johns Hopkins Burn Center, to some wounds as the control scaffold and, left others covered only with dressing.

Results and Discussion

Dextran Hydrogel Promotes Wound-Healing Process. Others have established that if burns primarily heal in less than 21 d, they exhibit minimal scar formation; whereas, if healing remains incomplete by 21 d, a satisfactory scar is unlikely (30). We analyzed the progress in wound healing at different time points along the 3 weeks after treatment application. We noticed a significant improvement in the survival of mice with wounds treated with hydrogel and control scaffold compared to mice treated with dressing

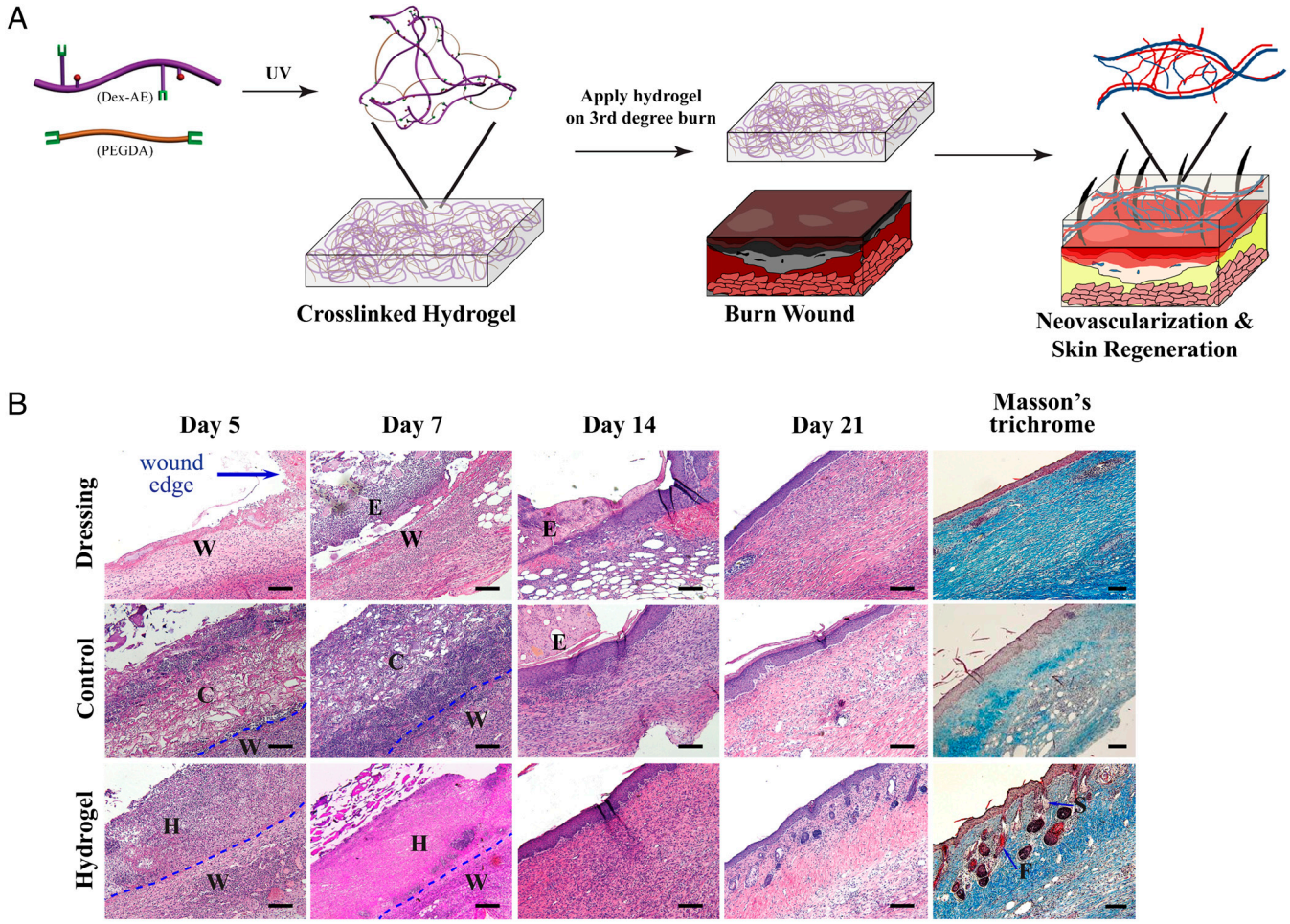

Fig. 1. Dextran hydrogel as a therapeutic modality. (*A*) Dextran-based hydrogel promotes neovascularization: Precise structure manipulation allows us to achieve rapid, efficient, and functional neovascularization. (*B*) Representative images of H&E-stained histological sections at time intervals show that dextran hydrogel promoted wound healing with complete skin appendage regeneration. Masson's trichrome staining indicates distinct collagen structures formed in dermal layer by day 21. Wound edge indicates the excision rim. W, wound area; H, hydrogel scaffold; C, control scaffold; E, eschar; F, follicle; S, sebaceous gland. Scale bars, 100 μm.

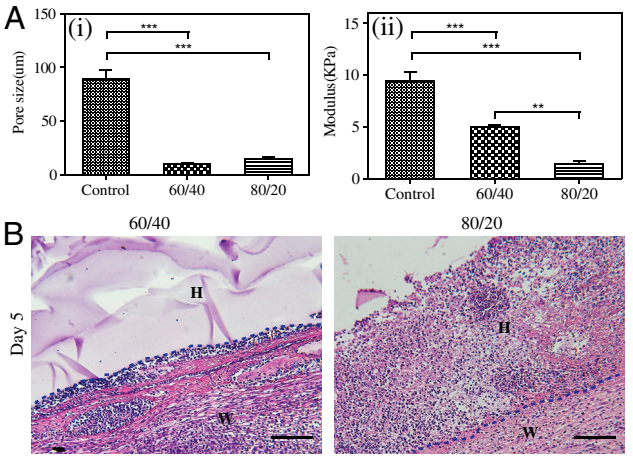

Fig. 2. Characterization of scaffold treatments. Dextran hydrogels (60/40 and 80/20) and cross-linked bovine tendon collagen and glycosaminoglycan scaffolds (control scaffold) were analyzed for (*A*) (*i*) porosity and (*ii*) mechanics. (*B*). Representative H&E-stained image on day 5 of low ratio (60/40) and high ratio (80/20). W, wound area; H, hydrogel scaffold. Scale bars, 100 μm.

alone (100% vs 60%, respectively; we did not observe differences in survival rate between mice treated with hydrogel and controlled scaffolds). Histological analysis revealed that, compared to wound healing when treated with the control scaffold, dextran hydrogel yielded an accelerated healing kinetics, which resulted in regenerated skin with a defined underlying collagen layer after 3 weeks of treatment (Fig. 1*B*; Fig. S1*B*).

To further understand how the dextran hydrogels promote healing better than control scaffolds, we performed additional burn studies that included two types of amine-modified dextran hydrogels—Dex-AE/ PEGDA in high (80/20) and low (60/40) ratios (26, 27). We found that both high- and low-ratio dextran hydrogels have a smaller pore size and are softer compared to control scaffolds. Although no significant difference in pore size was observed between the high and low-ratio dextran hydrogels, high-ratio dextran hydrogel scaffolds are significantly softer than low-ratio dextran hydrogels (Fig. 2*A*; Fig. S2*A*). From our in vivo

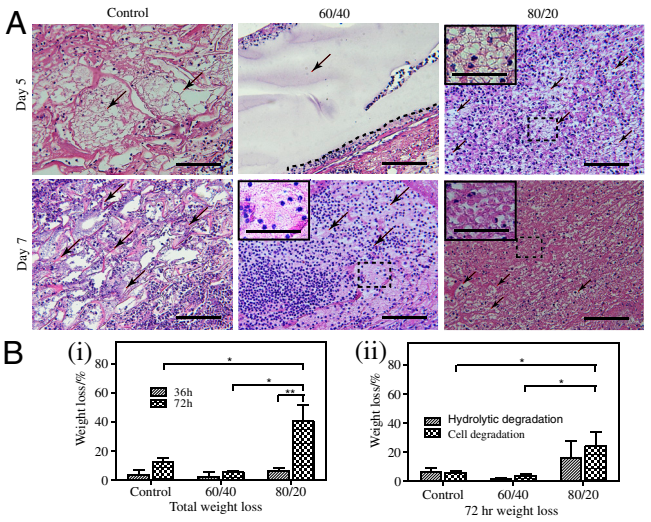

Fig. 3. Hydrogel degradation. (*A*) Representative images of H&E-stained histological sections of control scaffold (*Left*), low-ratio dextran hydrogel (*Center*), and high-ratio dextran hydrogel (*Right*) on days 5 and 7 of treatment show gel fragmentation (indicated by arrows and magnified inserts). (*B*) In vitro degradation of control scaffold and hydrogels measured by (*i*) the total change in scaffold mass and (*ii*) the relative contribution of HL60 cells and hydrolysis after 72 h. Scale bars, 100 μm (40 μm in insets).

studies ($n = 6$), we noticed that within 5 d high-ratio dextran hydrogel scaffolds (i.e., 80/20) facilitate accelerated cell infiltration compared to low-ratio dextran hydrogel scaffolds (Fig. 2*B*). In agreement with our previous findings (27), these results suggest that high-ratio dextran hydrogel scaffolds promote rapid wound healing due to their overall physical properties.

Hydrogel Degradation. Interestingly, after 7 d of treatment, we found a more fragmented gel structure in the wounds treated with high-ratio hydrogel scaffold compared to those treated with low-ratio hydrogel scaffold and control scaffold (Fig. 3*A*). As an acute inflammatory response is the first step in third-degree burn wound healing we performed, an in vitro degradation study to examine if inflammatory cells have any effect on the degradation. Both types of dextran hydrogel scaffolds and control scaffold cultured with inflammatory cells and their weight loss were measured. To distinguish between scaffold degradation by the cells and hydrolytic degradation process, we also incubated the scaffolds in cell culture media alone. We found that high-ratio dextran hydrogel scaffold was degraded more rapidly than low-ratio and control scaffold (Fig. 3*B*, *i*). Moreover, we found that both cells and hydrolysis accelerate the degradation of the high-ratio dextran hydrogel compared to low-ratio dextran hydrogel and control scaffold (Fig. 3*B*, *ii*). The slower degradation of the low-ratio dextran hydrogel was attributed to the higher content of nondegradable PEGDA and higher cross-linking density (26). In light of these data, we focused our analysis of burn wound-healing kinetics using high-ratio dextran hydrogel.

Inflammatory Cell Infiltration Expedites Hydrogel Degradation. Our in vitro data suggest that an efficient neutrophil penetration during the healing process of burn wounds may accelerate the degradation of the hydrogel more than control scaffold. Thus, to determine the contribution of the acute inflammatory response to hydrogel degradation, and the accelerated healing of wounds treated with dextran hydrogels, we analyzed wounds on day 5 following application of the dressing, which is when we first detected cellular penetration into the hydrogel. Although we could not detect differences in T-cell response, we did observe differences in the accumulation of macrophages and neutrophils between the control scaffold and dextran hydrogel ($n = 6$). Because neutrophil recruitment is a normal response in the wound area, more neutrophils were observed on day 7 than on day 5. Following the application of the control scaffold to the wound, we found that neutrophils congregated at the wound periphery

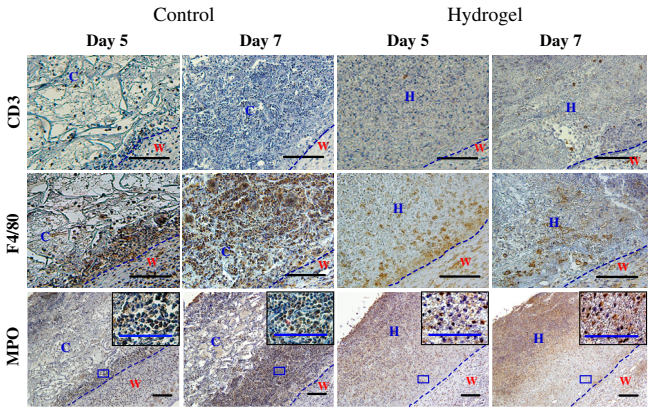

Fig. 4. Inflammatory cell infiltration. Histological sections of control scaffold-treated and hydrogel-treated wounds (*Left* and *Right*, respectively) on days 5 and 7 of treatment, stained for CD3 (T cell), F4/80 (macrophage), and MPO (neutrophil). High magnification corresponds to boxed area in the low-magnification images. The dotted line represents the interface between wound and dressing (control scaffold or hydrogel). W, wound area; H, hydrogel scaffold; C, control scaffold. Scale bars, 100 μm.

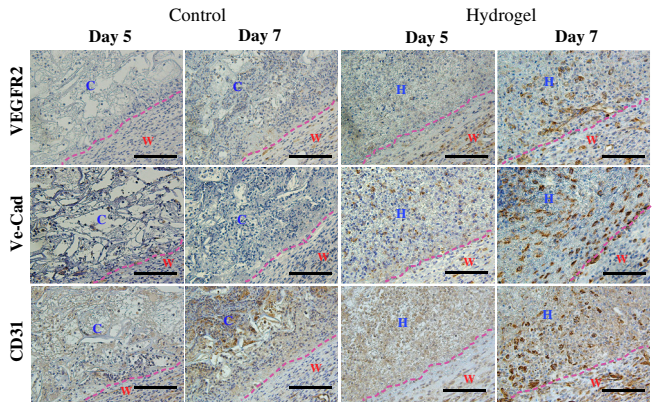

Fig. 5. Angiogenic cell infiltration. Histological sections of control scaffold-treated and hydrogel-treated wounds (*Left* and *Right*, respectively) on days 5 and 7 of treatment, stained for VEGFR2 (*Top*), VE-Cad (*Middle*), and CD31 (*Bottom*). The dotted line represents the interface between wound and control scaffold or hydrogel. W, wound area; H, hydrogel scaffold; C, control scaffold. Scale bars, 100 μm.

by day 5; on day 7, we observed increased neutrophil accumulation at the wound area, generating a thicker layer at the interface of the wound and the treatment area (Fig. 4). In the case of dextran hydrogel scaffold, neutrophils infiltrated into the hydrogel scaffolds by day 5 and continued on day 7, resulting in less neutrophil aggregation at the periphery (Fig. 4; Fig. S3). Indeed, the different response of neutrophils in wounds treated with hydrogels resulted in an almost complete digestion of the hydrogel by day 7 after implantation; however, in the control group, large fragmented sections of the scaffolds remained undigested (as shown above in Fig. 3*A*). This data further confirmed that in addition to hydrolysis, efficient inflammatory cell penetration during the healing process of burn wounds accelerated the degradation of the hydrogel more than control scaffold. Our data agrees with the results of another study suggesting that neutrophils promoted chitosan hydrogel degradation (23). Additionally, recent studies demonstrated that a degradable hydrogel allowed and directed cell growth in vitro (31, 32) compared to nondegradable hydrogels. Altogether, we suggest that a distinctive hydrogel structure, which enables rapid hydrogel degradation, promotes the healing process of third-degree burn wounds by accelerating disintegration of the scaffold during the repair phase.

Angiogenic Cells Home to Dextran Hydrogel. We proceeded to examine the angiogenic response, the next step in the burn-healing process. Vascular endothelial growth factor receptor 2 (VEGFR2) is a known marker for endothelial progenitor cells (33, 34) and is involved in angiogenic processes (35, 36). In burn wounds treated with hydrogel, we detected cells positive for VEGFR2 and luminal structure formation by day 5. We could not detect cells positive for VEGFR2 in burn wounds treated with control scaffold (Fig. 5, *Top*). Moreover, we observed early vascular networks within the hydrogel area on day 5, as evidenced by positive CD31 staining. These networks expanded and developed by day 7 after implantation in the case of hydrogels, but these networks were not observed in the control scaffold -treated wounds (Fig. 5, *Middle*). We could also detect vascular endothelial cadherin (VE-Cad)-positive networks on day 7 after hydrogel placement (Fig. 5, *Bottom*). Previous clinical (37, 38) and animal model studies (1) revealed an increased number of circulating angiogenic cells after burn injuries and found that angiogenesis played a critical role in wound repairs. Our results indicate that dextran hydrogels, unlike control scaffolds, accelerated the recruitment of endothelial progenitors and cells to the wound area, enabling rapid neovascularization after a week of treatment.

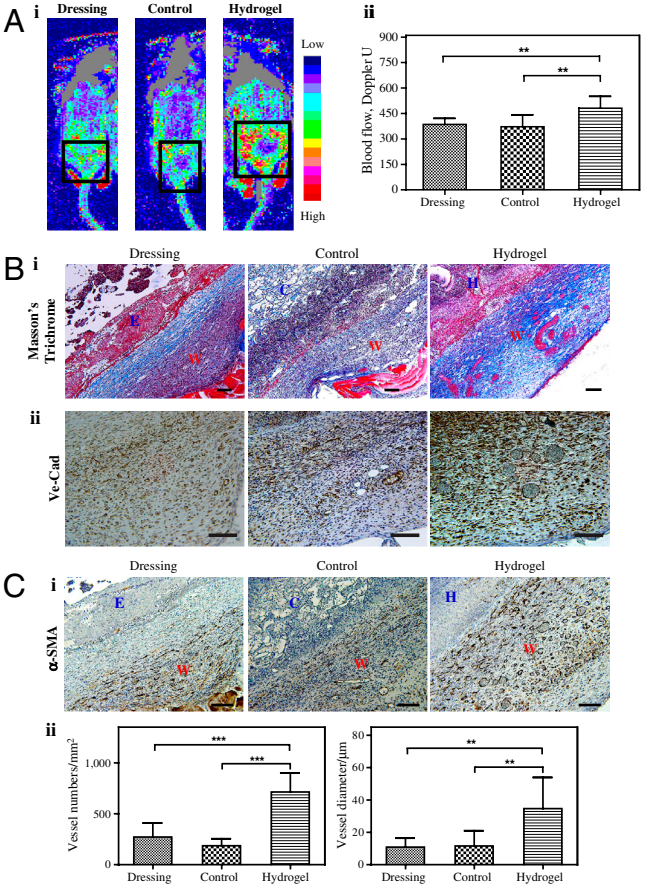

Fig. 6. Angiogenic response in day 7. (*A*) Doppler images of angiogenic response to wound injuries (*i*), and quantification (*ii*).The square indicates the wound area under Doppler. (*B*) Masson's staining (*i*) and VE-Cad staining (*ii*) of wound sites. Collagen layers were formed on the control (untreated) wounds, whereas no such layers formed on control scaffold-treated and hydrogel-treated wounds by day 7; we observed functional blood cells in the hydrogel-treated wounds. (*C*) Photo of α-SMA staining (*i*) and quantification based on α-SMA staining (*ii*) of the wound areas. W, wound area; E, eschar; H, hydrogel scaffold; D, dressing; C, control scaffold. Significance levels were set at: $*p < 0.05$, $**p < 0.01$, and $***p < 0.001$. Values shown are means ± SD. Scale bars, 100 μm.

Dextran Hydrogel Promotes Angiogenic Response. To better determine the functionality of the developing vasculature, we analyzed wounds on day 7, using laser Doppler to assess blood flow surrounding the wound, and immunohistochemical analysis to quantify the new vascular networks within wounds. We attempted to determine the blood flow within the wound area; however, having covered the wounds with the dressing, they were not accessible to allow accurate measurement by the laser Doppler, and removing the dressing ruptured the healing tissue. Therefore, we performed laser Doppler in the boundary area, as illustrated in Fig. S4 ($n = 4$). We found that by day 7, dextran hydrogels induced more blood flow to the burn wound area than did the control scaffold and the wound covered with only dressing (Fig. 6*A*, *i*). For example, the blood flow with hydrogel was 481 perfusion units, whereas the blood flow was only 385 perfusion units and 372 perfusion units for dressing-covered control and control scaffold, respectively (Fig. 6*A*, *ii*). We observed no significant difference between control scaffold-treated wounds and dressing-covered controls, suggesting that the control scaffold fails to promote angiogenesis in the wound boundary area. To investigate angiogenesis within the wound, we used Masson's trichrome staining, which revealed an increase in delineated vascular networks and the formation of a collagen layer in wounds

covered with hydrogels (Fig. 6*B*, *i*), further confirmed with specific staining for vascular networks (Fig. 6*B*, *ii*). To identify vascular networks stabilized with smooth muscle cells (SMCs), we stained for alpha-smooth muscle actin (α-SMA); we found that wounds treated with hydrogels demonstrated a significant increase in vascular networks layered with SMCs (Fig. 6*C*, *i*). For instance, wounds covered with hydrogel had approximately 714 blood vessels per square millimeter, whereas we found only 271 and 182 blood vessels per square millimeter for dressing-covered wounds and wounds treated with control scaffold, respectively (Fig. 6*C*, *ii*). These data support the Doppler analysis findings of increased blood flow around healing wounds treated with hydrogels, demonstrating enhanced vessel growth into the hydrogels compared to control scaffold.

Dextran Hydrogel Results in Complete Skin Regeneration. Finally, we analyzed the structure of the regenerated skin. As mentioned above, we observed healing within 3 weeks of wound cover. Indeed, at this time point, regression of the vasculature allowed dermal maturation accompanied skin regeneration. We analyzed the regenerating skin structure for epithelial maturation, dermal differentiation, and hair follicles (39). The results showed that the dextran hydrogel promoted significant skin maturation; hydrogel-treated wounds had a mature epithelial structure with hair follicles and sebaceous glands ($n = 6$) (Fig. 7*A*, *i* and *ii*; Fig. S5). Moreover, we observed a significant increase in the number of hair follicles (Fig. 7*A*, *iii*). Indeed, when the treatment continued for extended periods, we observed hair growth in the center of hydrogel-treated wounds (Fig. 7*B*). In addition, quantification of the skin thickness revealed that the hyperplastic regenerating skin is being remodeled after 3 weeks of treatment, and reaches the thickness of normal mouse skin by 5 weeks of treatment (Fig. 7*C*; Fig. S6). Ito et al. demonstrated that nascent follicles arise from epithelial cells outside of the hair follicle stem cell niche, suggesting that epidermal cells in the wound assume a hair follicle stem cell phenotype (40). We demonstrated epithelial repair within 14 d of hydrogel application, and mature epithelial morphology with hair follicles and sebaceous glands after 21 d. These results may suggest that the hydrogel facilitate epithelial cell migration or homing to the wound area and support epithelial differentiation.

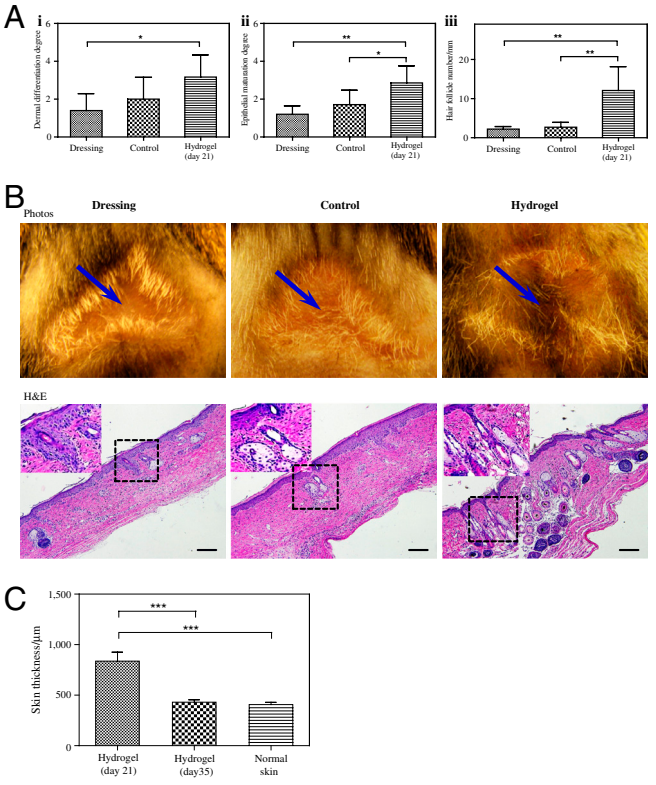

Fig. 7. Evaluation of regenerated skin structures. (*A*) Quantification of skin structures in terms of dermal differentiation (*i*), epithelial maturation (*ii*), and the number of hair follicles (*iii*). (*B*) A 5-week-long study further demonstrated that dextran hydrogels promote complete skin regeneration with new hair growth, as shown by photos (arrows indicate the center of the original wound; *Upper*) and H&E-stained histologic sections. High magnification corresponds to boxed area in the low-magnification images. (*C*) Quantification of skin thickness after 3-week and 5-week-long treatment compared to normal mouse skin. Significance levels were set at: $*p < 0.05$, $**p < 0.01$, and $***p < 0.001$. Values shown are means ± SD. Scale bars, 100 μm.

Functional neovascularization, which facilitates cell and nutrition transportation as well as oxygen exchange, is critical for perfect skin regeneration. In our study, the distinctive hydrogel structure facilitates neutrophil infiltration, neutrophils facilitate hydrogel digestion, and this leads to vascular cell infiltration. Thus, unlike the clinically used scaffold, dextran hydrogels accelerate the recruitment of endothelial cells to the wound area, enabling rapid neovascularization after a week of treatment. The wound treated hydrogel resulted in skin regeneration with appendages (hair follicles and sebaceous glands). Overall, our study clearly demonstrates that dextran hydrogel alone, without the addition of growth factors or cytokines, promotes rapid neovascularation and complete skin regeneration, thus holding great potential to serve as a unique device for superior treatment of dermal wounds in clinical applications.

Materials and Methods

A detailed description of the materials and methods is available in *SI Materials and Methods*.

Surgery Procedure. The Johns Hopkins University Animal Care and Use Committee approved all procedures. We anesthetized mice by intraperitoneal injection of ketamine hydrochloride and xylazine hydrochloride; then we shaved the dorsum and applied a depilatory (Nair; Church & Dwight Co, Inc.). The burn injury was generated as previously reported (1). Briefly, a custom-made 220-g aluminum rod was heated in a 100 °C water bath for 5 min. We used a template (1.2-cm diameter) to place the wounds on the posterior-dorsum of each mouse for 4 s. We resuscitated the mice by intraperitoneal injection of saline, using half of the Parkland Formula (4 mL/kg × percent body area), within 1 h after burning.

To follow current clinical practice, we performed burn wound excisions after 48 h. We removed full-thickness skin and generated an 8-mm-diameter round wound, and covered the wounds with the same size of dextran hydrogels or Integra (control scaffold; both with thickness of approximately 1 mm) and applied DuoDerm dressing. Some wounds were only covered with DuoDerm dressing (dressing-covered control).

Laser Doppler Analysis. We measured blood flow in wound areas using a scanning laser Doppler imager (Model LDI2-IR, Moor Instruments) with a near-infrared laser diode at 785 nm. The imaging system uses a low-power (2 mW) infrared laser beam to sequentially scan the tissue at several thousand measurement points. For each measurement point, a signal is generated that scales linearly with tissue perfusion, defined as the product of the blood cell velocity and concentration. This signal, termed the "laser Doppler perfusion index" (LDPI), was represented as a two-dimensional color image on a computer screen. The colors produced illustrate the spectrum of perfusion in the wound: Dark blue depicts the lowest level of perfusion and red the highest. The system simultaneously produced a photographic image, allowing the direct anatomical comparison of corresponding areas of burn. For each burn, the area of interest was selected by drawing free hand after exporting the image into the software package (the Moor LDI V5.2 software). Then, the mean LDPI value within this area of interest was computed. The scanner was positioned 32 cm above each animal, and scans were performed on day 7 to assess blood flow in the wound margin area. Because of its measurement limits, the Doppler cannot determine the blood flow under either hydrogel or Integra. Thus, we only examined the blood flow in the tissue-scaffold interface in each wound.

Skin Maturity Quantification. The skin structure on day 21 was assessed using H&E-stained histologic sections, according to previously published methods (39). At 21 d after the burn, we used specific criteria to assess each wound histologically for the number of hair follicles, epithelial maturation, and dermal differentiation. For epithelial maturation, the grading was defined according to the following criteria: grade 1, thin and with no reticulation; 2, occasional reticulation; 3, moderate reticulation; 4, thick and with complex reticulation. The grading for dermal differentiation used the following criteria: grade 1, thin, dense, and monotonous fibrosis; 2, thicker but still dense and monotonous fibrosis; 3, two layers but not completely discreet; 4, two discreet layers with superficial fibrosis and loose alveolar tissue within the deep layer. We counted hair follicles as the number within the wound, between the terminal ends of the panniculus carnosus muscle. Skin thickness was determined by measuring the epidermis, dermis, and fat tissue in H&E-stained histologic sections and Masson's trichrome-stained histologic sections.

ACKNOWLEDGMENTS. We thank Prof. Jason Burdick for critical review of the manuscript. This research was partially funded by the Maryland Stem Cell Research Fund Postdoctoral Fellowship (to G.S.), the Maryland Stem Cell Research Fund (to J.W.H. and S.G.), and by National Institutes of Health Grant R01HL107938 (to S.G.).

1. Zhang X, et al. (2010) Association of increasing burn severity in mice with delayed mobilization of circulating angiogenic cells. *Arch Surg* 145:259–266.
2. Sen S, Greenhalgh D, Palmieri T (2010) Review of burn injury research for the year 2009. *J Burn Care Res* 31:836–848.
3. Fagenholz PJ, Sheridan RL, Harris NS, Pelletier AJ, Camargo CA, Jr (2007) National study of Emergency Department visits for burn injuries, 1993 to 2004. *J Burn Care Res* 28:681–690.
4. Zhang X, et al. (2010) Impaired angiogenesis and mobilization of circulating angiogenic cells in HIF-1α heterozygous-null mice after burn wounding. *Wound Repair Regen* 18:193–201.
5. Kirker KR, Luo Y, Nielson JH, Shelby J, Prestwich GD (2002) Glycosaminoglycan hydrogel films as bio-interactive dressings for wound healing. *Biomaterials* 23:3661–3671.
6. Gurtner GC, Werner S, Barrandon Y, Longaker MT (2008) Wound repair and regeneration. *Nature* 453:314–321.
7. Li J, Zhang Y-P, Kirsner RS (2003) Angiogenesis in wound repair: Angiogenic growth factors and the extracellular matrix. *Microsc Res Tech* 60:107–114.
8. Martin P (1997) Wound healing—Aiming for perfect skin regeneration. *Science* 276:75–81.
9. Tibbs MK (1997) Wound healing following radiation therapy: A review. *Radiother Oncol* 42:99–106.
10. Haroon ZA, Hettasch JM, Lai T-S, Dewhirst MW, Greenberg CS (1999) Tissue transglutaminase is expressed, active, and directly involved in rat dermal wound healing and angiogenesis. *FASEB J* 13:1787–1795.
11. Steed DL (1997) The role of growth factors in wound healing. *Surg Clin North Am* 77:575–586.
12. Kim M-H, et al. (2008) Dynamics of neutrophil infiltration during cutaneous wound healing and infection using fluorescence imaging. *J Invest Dermatol* 128:1812–1820.
13. Greenhalgh DG (1998) The role of apoptosis in wound healing. *Int J Biochem Cell Biol* 30:1019–1030.
14. Singer AJ, Clark RAF (1999) Cutaneous wound healing. *N Engl J Med* 341:738–746.
15. Tredget EE (2007) The basis of fibrosis and following thermal injury wound healing disorders. *J Trauma* 62:S69–S69.
16. Boucard N, et al. (2007) The use of physical hydrogels of chitosan for skin regeneration following third-degree burns. *Biomaterials* 28:3478–3488.
17. Kiyozumi T, et al. (2007) The effect of chitosan hydrogel containing DMEM/F12 medium on full-thickness skin defects after deep dermal burn. *Burns* 33:642–648.
18. Kim KL, et al. (2009) Enhanced dermal wound neovascularization by targeted delivery of endothelial progenitor cells using an RGD-g-PLLA scaffold. *Biomaterials* 30:3742–3748.
19. Madsen J, et al. (2008) Biocompatible wound dressings based on chemically degradable triblock copolymer hydrogels. *Biomacromolecules* 9:2265–2275.
20. Shepherd J, et al. (2011) Hyperbranched poly(NIPAM) polymers modified with antibiotics for the reduction of bacterial burden in infected human tissue engineered skin. *Biomaterials* 32:258–267.
21. Balakrishnan B, Mohanty M, Umashankar PR, Jayakrishnan A (2005) Evaluation of an in situ forming hydrogel wound dressing based on oxidized alginate and gelatin. *Biomaterials* 26:6335–6342.
22. Puolakkainen PA, et al. (1995) The enhancement in wound healing by transforming growth factor-[beta]1 (TGF-[beta]1) depends on the topical delivery system. *J Surg Res* 58:321–329.
23. Kiyozumi T, et al. (2006) Medium (DMEM/F12)-containing chitosan hydrogel as adhesive and dressing in autologous skin grafts and accelerator in the healing process. *J Biomed Mater Res B Appl Biomater* 78B:129–136.
24. Liu SQ, Rachel Ee PL, Ke CY, Hedrick JL, Yang YY (2009) Biodegradable poly(ethylene glycol)-peptide hydrogels with well-defined structure and properties for cell delivery. *Biomaterials* 30:1453–1461.
25. Lee PY, Cobain E, Huard J, Huang L (2007) Thermosensitive hydrogel PEG-PLGA-PEG enhances engraftment of muscle-derived stem cells and promotes healing in diabetic wound. *Mol Ther* 15:1189–1194.
26. Sun G, Shen Y-I, Ho CC, Kusuma S, Gerecht S (2010) Functional groups affect physical and biological properties of dextran-based hydrogels. *J Biomed Mater Res A* 93A:1080–1090.
27. Sun G, et al. (2011) Functional neovascularization of biodegradable dextran hydrogels with multiple angiogenic growth factors. *Biomaterials* 32:95–106.
28. Light TD, et al. (2004) The 2003 Carl A Moyer Award: Real-time metabolic monitors, ischemia-reperfusion, titration endpoints, and ultraprecise burn resuscitation. *J Burn Care Rehabil* 25:33–44.
29. Schulz JT, III, Tompkins RG, Burke JF (2000) Artificial skin. *Annu Rev Med* 51:231–244.
30. Cubison TCS, Pape SA, Parkhouse N (2006) Evidence for the link between healing time and the development of hypertrophic scars (HTS) in paediatric burns due to scald injury. *Burns* 32:992–999.
31. Khetan S, Katz JS, Burdick JA (2009) Sequential crosslinking to control cellular spreading in 3-dimensional hydrogels. *Soft Matter* 5:1601–1606.
32. Kloxin AM, Kasko AM, Salinas CN, Anseth KS (2009) Photodegradable hydrogels for dynamic tuning of physical and chemical properties. *Science* 324:59–63.
33. Peichev M, et al. (2000) Expression of VEGFR-2 and AC133 by circulating human CD34+ cells identifies a population of functional endothelial precursors. *Blood* 95:952–958.
34. Sibal L, et al. (2009) Circulating endothelial progenitor cells, endothelial function, carotid intima-media thickness and circulating markers of endothelial dysfunction in people with type 1 diabetes without macrovascular disease or microalbuminuria. *Diabetologia* 52:1464–1473.
35. Flamme I, Breier G, Risau W (1995) Vascular endothelial growth factor (VEGF) and VEGF receptor 2(flk-1) are expressed during vasculogenesis and vascular differentiation in the quail embryo. *Dev Biol* 169:699–712.
36. Sase H, Watabe T, Kawasaki K, Miyazono K, Miyazawa K (2009) VEGFR2-PLCγ1 axis is essential for endothelial specification of VEGFR2+ vascular progenitor cells. *J Cell Sci* 122:3303–3311.
37. Fox A, et al. (2008) Mobilization of endothelial progenitor cells into the circulation in burned patients. *Br J Surg* 95:244–251.
38. Gill M, et al. (2001) Vascular trauma induces rapid but transient mobilization of VEGFR2+AC133+ endothelial precursor cells. *Circ Res* 88:167–174.
39. Ehrbar M, et al. (2004) Cell-demanded liberation of VEGF121 from fibrin implants induces local and controlled blood vessel growth. *Circ Res* 94:1124–1132.
40. Ito M, et al. (2007) Wnt-dependent de novo hair follicle regeneration in adult mouse skin after wounding. *Nature* 447:316–320.